

## Surface Properties of CdS Nanoparticles

P. P. Favero, M. de Souza-Parise, J. L. R. Fernandez, R. Miotto,

*Instituto de Física da Universidade de Brasília, Caixa Postal 04455, CEP 70919-970, Brasília, DF, Brazil*

and A. C. Ferraz

*Instituto de Física da Universidade de São Paulo, Caixa Postal 66318, CEP 05315-970, São Paulo, SP, Brazil*

Received on 8 December, 2005

With a view to contribute to the understanding the surface effects on optical properties process, and its hole in the electronic properties of the nanoparticles, CdS based nanoparticles are characterised by different experimental techniques and the experimental results compared to density functional theory calculations. Our results indicate that cubic CdS nanoparticles present a strong structural deformation, hexagonal reconstructed structures preserve their lattice behaviour. Both cubic and hexagonal CdS nanoparticles are S-terminated after relaxation, even when mildly Cd-rich nanoparticles are considered. A broad peak observed in our PL measurements is interpreted as an experimental evidence of the surface related peak observed around 1.8 eV in our calculated DOS for the hexagonal relaxed structure.

Keywords: CdS; Nanoparticles; Electronic structure; Photoluminescence

### I. INTRODUCTION

The development of new synthesis techniques for the production of semiconductor nanoparticle materials showing quantum size effects [1] has attracted the attention of a great number of experimental and theoretical groups not only due to the understanding of its fundamental aspects, but also to its importance in various technological applications, such as: Q-dots [2], probes for irregular DNA structures [3], fluorescence probes in peptides detection [4], among others. As expected, each of these needs requires the development of a well defined organic layer on the nanoparticle surface. Indeed, surfactant coating, primarily used to stabilise nanoparticles and hence to avoid their permanent aggregation, are now been designed in order to guarantee site selectivity, specially in biochemical applications, such as drug carriers. In this sense, a systematic study of the nanoparticle surface sites and its interaction with different functional groups is crucial in order to contribute to a better control and production of such devices.

In addition to its size/volume ratio, the distribution of charge over the surface was found to be a key issue in the application of nanoparticles as components of semiconductor electrodes [5]. Absorption and photocurrent investigations on CdS nanoparticle modified electrodes [6] indicates that surface states might play a crucial role in the device performance. Alternatively, the origin of deep levels inside the bulk bandgap, may be related to defects inside the bulk or impurities incorporated during the chemical process of nanoparticle synthesis. With a view to contribute in this discussion, in this work, CdS nanoparticles are synthesised by a chemical route and are characterised by photoluminescence spectroscopy, X-ray, and transmission electron microscopy. The experimental results for the electronic structure are then compared to density functional calculations.

### II. EXPERIMENTAL AND THEORETICAL MODELLING

Photoluminescence (PL) measurements were performed using a commercial triple spectrometer (Jobin Yvon Model T64000) equipped with a GaAs detector. The 488 nm line from a CW Argon ion laser was used to illuminate the samples. All measurements were performed at room temperature, at an optical power of the order of 10 mW. The particle size polydispersity profile of the sample was obtained from the transmission electron microscopy (TEM) micrographs using a Jeol 100CXII system. A digitiser was used to obtain the particle diameter from the TEM pictures.

The CdS nanoparticles were prepared as follow: cadmium nitrate was purchased from VETEC and used as received without further purification. The nanoparticles were synthesised in an aqueous solution of  $(\text{NH}_4)_2\text{S}$  and  $\text{Cd}(\text{NO}_3)_2$ , prepared separately and quickly mixed to form a CdS nanocrystal. After precipitation, the nanoparticles were centrifuged and dried in vacuum. The samples were prepared considering a Cd:S molar concentration of 0.85.

To gain further physical insight into the available experimental data, we employ the density functional theory to investigate the structural and electronic properties of a series of nanoparticles in their cubic and hexagonal reconstructions. We have considered different sized hexagonal (cubic) nanoparticles, namely  $\text{Cd}_8\text{S}_5$ ,  $\text{Cd}_{20}\text{S}_{16}$ , and  $\text{Cd}_{28}\text{S}_{28}$  ( $\text{Cd}_{16}\text{S}_{14}$ ,  $\text{Cd}_{28}\text{S}_{25}$ , and  $\text{Cd}_{42}\text{S}_{44}$ ), corresponding to spherical symmetric structures of 1.0, 1.3 and 1.5 nm respectively. The theoretical values of the bulk CdS lattice constants in its hexagonal and cubic phases were used in the nanoparticles calculations. The electron-ion interaction between the Cd and S atoms is described by PAW potentials [7, 8] and the electron-electron exchange-correlation interactions were considered by using a generalised gradient approximation (GGA) [9] of the density functional theory. The single-particle orbitals were expressed in a plane-wave basis up to the kinetic energy of 280 eV, whereas the cutoff for the augmentation charges is 456 eV. Increasing the energy cut-off to 310 eV did

not change the key structural parameters by more than 0.4%. The difference between total energy values calculated using both plane wave expansions are smaller than 0.1%. The electronic and ionic degrees of freedom were relaxed by adopting the Vienna Ab-initio Simulation Package (VASP) implementation [10]. For the Brillouin-zone summation, a single special  $\mathbf{k}$  points was used for all nanoparticles calculations. The atoms were assumed to be in their fully relaxed positions when the forces acting on the ions were smaller than 0.01 eV/Å. The relaxed adsorption geometries were used to calculate the zone-centre vibrational modes within a restricted dynamical matrix scheme [11]. For setting up the dynamical problem we have considered only surface atoms.

### III. RESULTS AND DISCUSSION

After production, the CdS nanoparticles were characterised by TEM and X-ray measurements. From the electron microscopy data we obtained the average particle diameter ( $d = 10$  nm) and the diameter dispersity (0.3), using a log-normal distribution function to fit the TEM data. A similar average particle diameter was obtained via X-ray measurements that also indicate the hexagonal cristaline structure of our samples.

For bulk CdS our first-principles calculations produced  $a_0 = 5.88$  Å for the cubic phase and  $a = 4.11$  Å and  $c = 6.74$  Å for the hexagonal lattice, all in good agreement with the experimental ( $a_0 = 5.83$  Å  $a = 4.13$  Å and  $c = 6.75$  Å) values presented in Ref. [12]. The hexagonal and cubic nanoparticles derived from our bulk calculations are presented in Figs. 1 and 2, respectively. Following a conjugate-gradient algorithm, the six unrelaxed configurations, showed at the upper panels of Figs. 1 and 2 were submitted to the search of a minimum energy state whose final reconstructed structures are presented on the bottom panels. Both 1.0 nm CdS nanoparticles ( $\text{Cd}_8\text{S}_5$  and  $\text{Cd}_{16}\text{S}_{14}$ ), present a strong structural deformation, which is a possible indication of a molecular behaviour dominance over the cristaline structure. By comparing Figs. 1 and 2 we conclude that the transition from a molecular behaviour to nanoparticles with cristaline core is first observed for the hexagonal phase structure. Indeed, the 1.3 nm hexagonal nanoparticle ( $\text{Cd}_{20}\text{S}_{16}$ ) shows a lattice pattern preservation, not clearly observed even for the 1.5 nm cubic nanoparticle ( $\text{Cd}_{42}\text{S}_{44}$ ).

It is also interesting to note, that for all considered nanoparticles, regardless their lattice phase and size, surface Cd atoms tend to migrate to the sub-surface layer. In other words, for Cd rich samples ( $\text{Cd}_8\text{S}_5$ ,  $\text{Cd}_{16}\text{S}_{14}$ ,  $\text{Cd}_{20}\text{S}_{16}$ ,  $\text{Cd}_{28}\text{S}_{25}$ ), neutral samples ( $\text{Cd}_{28}\text{S}_{28}$ ) and S rich ( $\text{Cd}_{42}\text{S}_{44}$ ), all considered nanoparticles are S terminated. This is in agreement with the experimental X-ray photoelectron spectroscopy (XPS) observations by Winkler and co-workers [13], who clearly indicates that the different sized CdS nanoparticles, with a molar ratio 1:1, investigated by them are S-terminated. This is against the most accepted nanoparticle synthesis process, as it assumes that when the molar ratio of Cd and S ions is 1:1 the surface of CdS nanoparticles is neutral, while surface-rich  $\text{Cd}^{2+}$  or  $\text{S}^{2-}$  CdS nanoparticles are obtained by adding excessive Cd

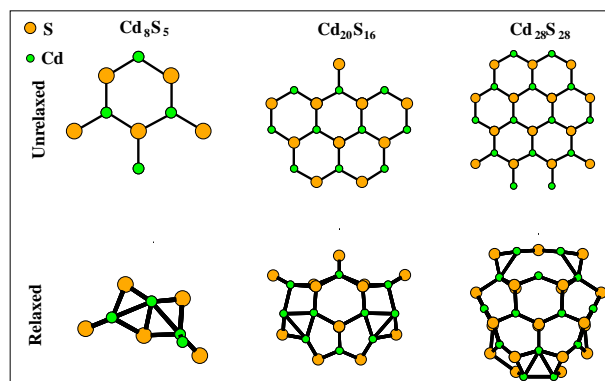


FIG. 1: Representation of (a) unrelaxed and (b) relaxed hexagonal CdS nanoparticles.

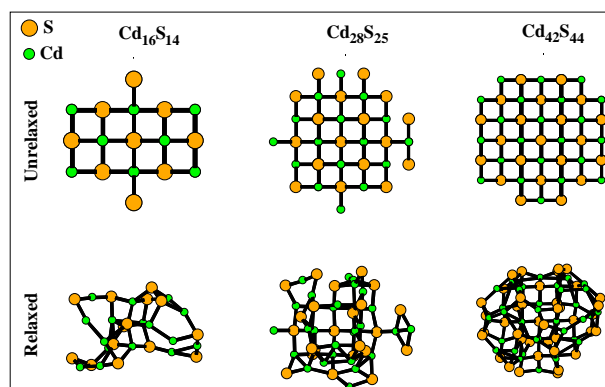


FIG. 2: Representation of (a) unrelaxed and (b) relaxed cubic CdS nanoparticles.

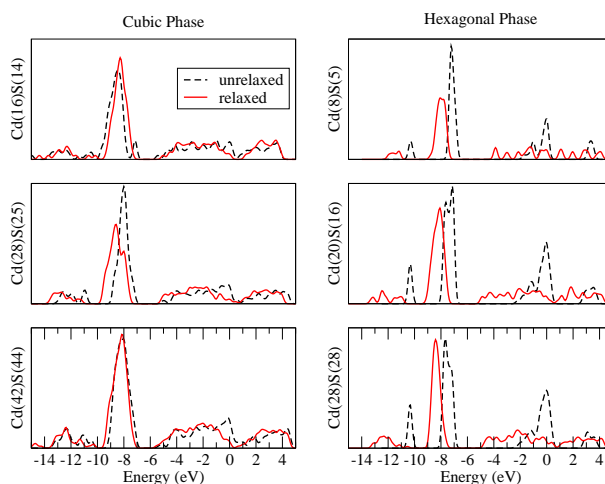


FIG. 3: Electronic density of states (DOS) of the cubic and hexagonal CdS nanoparticles before (dashed lines) and after (solid lines) relaxation. The zero of energy is aligned with the top of the valence band.

(Cd:S = 2:1) or S (Cd:S=1:2) [14].

In the next step of our analysis, we investigate the electronic structure of all considered nanoparticles. In Fig. 3 we present the electronic density of states (DOS) of the cubic and hexagonal CdS nanoparticles before (dashed lines) and after (solid lines) relaxation. All considered unrelaxed cubic nanoparticles present a quasimetallic character, i.e., the density of states are continuous with no clear gap at the Fermi level. After the relaxation/reconstruction process, a small band gap is observed, but the presence of surface states are not clear.

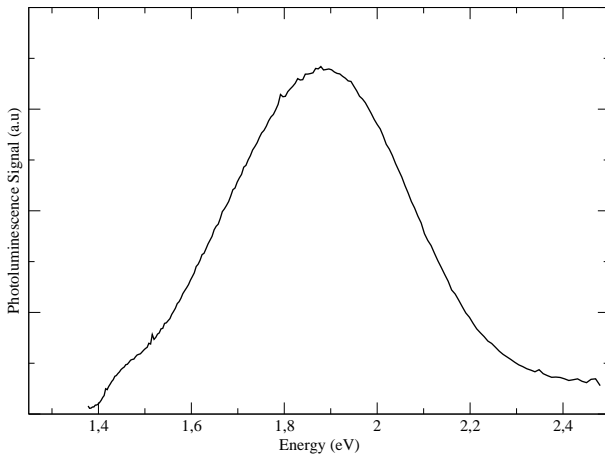


FIG. 4: Luminescence emission spectra of a 10.0 nm CdS nanoparticle, with a Cd:S molar ratio of 0.85.

The hexagonal unrelaxed nanoparticles, on the other hand, present a clear band gap region that decreases when the nanoparticles size increases, in agreement with experimental observations [5]. Upon relaxation, the semiconducting nature of the nanoparticle is preserved, but the main gap is substantially smaller. Our calculations indicate that this is a consequence of the presence of new surface related electronic states in the main gap region. We have also observed that the relaxed hexagonal structures present a DOS peak around 1.8 eV, that becomes more pronounced when the size of the

nanoparticle increases from 1.0 to 1.3 nm. However, for the 1.5 nm nanoparticle, the same peak presents a broaden band character. In order to check out the existence of such a peak, we present in Fig. 4 Luminescence emission spectra of a 10.0 nm CdS nanoparticle, with a Cd:S molar ratio of 0.85. Due to technical limitations from our apparatus, energies below 1.4 eV are not accessible. For the same reason, the shoulder observed in the 1.4-1.5 eV region can not be considered to be related to an energy level. A broad band, centred around 1.85 eV, is clearly observed. The broadening of the band is probably related to the size distribution of the CdS nanoparticles as it is well established that the main gap for these structures is highly influenced by its size. Therefore, we believe that this broad peak can be interpreted as an experimental evidence of the surface related peak observed around 1.8 eV in our calculated DOS for the hexagonal relaxed structure.

#### IV. CONCLUSIONS

From TEM and X-ray measurements, luminescence and Raman spectroscopy, combined with first-principles calculations, we have shown that while cubic CdS nanoparticles present a strong structural deformation, hexagonal reconstructed structures preserve their lattice behaviour. Both cubic and hexagonal CdS nanoparticles are S-terminated after relaxation, even when mildly Cd-rich nanoparticles are considered. A broad peak observed in our PL measurements is interpreted as an experimental evidence of the surface related peak observed around 1.8 eV in our calculated DOS for the hexagonal relaxed structure.

#### Acknowledgements

The authors acknowledge financial support from the Brazilian agencies CAPES, CNPq, and DPP-UnB. J. L. R. Fernandez is supported by CNPq (process number 503533/2003-3).

- 
- [1] Tito Trindade, Paulo O'Brien, and Nigel L. Pickett, *Chem. Mater.* **13**, 3843 (2001).
  - [2] Rachel P. Doherty, Stephen G. Hickey, D. Jason Riley, and Elizabeth J. Tull, *J. Electroanal. Chem.* **569**, 271 (2004).
  - [3] K. K. Caswell, Rahina Mahtab, and Catherine J. Murphy, *J. Fluorescence* **14**, 407 (2004).
  - [4] Xudong Chen, Xinbo Wang, Lin Liu, Dacheng Yang, and Li Fan, *Analytica Chimica Acta* **542**, 144 (2005).
  - [5] D. J. Riley and E. J. Tull, *J. Electroanal. Chem.* **504**, 45 (2004).
  - [6] Stephen G. Hickey, D. Jason Riley, and Elisabeth J. Tull, *J. Phys. Chem. B* **104**, 7623 (2000).
  - [7] P. E. Blöchl, *Phys. Rev. B* **50**, 17953 (1994).
  - [8] G. Kresse and J. Joubert, *Phys. Rev. B* **59**, 1758 (1999).
  - [9] J. P. Perdew, K. Burke, and M. Ernzerhof, *Phys. Rev. Lett.* **77**, 3865 (1996).
  - [10] G. Kresse and J. Furthmüller, *Comput. Mater. Sci.* **6**, 15 (1996).
  - [11] G. P. Srivastava, *The Physics of Phonons* (Adam Hilger, Bristol, 1990).
  - [12] D. R. Lide, *Handbook of Chemistry and Physics* (Chemical Rubber Company, Roca Raton, 1995).
  - [13] U. Winkler, D. Eich, Z. H. Chen, R. Fink, S. K. Kulkarni, and E. Umbach, *Chem. Phys. Lett.* **306**, 95 (1999).
  - [14] L. Jiang, B. Q. Yang, Y. D. Ma, Y. C. Liu, W. S. Yang, T. J. Li, and C. C. Sun, *Chem. Phys. Lett.* **380**, 29 (2003).